CHEMICAL ENGINEERING TRANSACTIONS
VOL. 73, 2019
A publication of AIDIC
The Italian Association of Chemical Engineering
Online at www.aidic.it/cet
Guest Editors: Andrea D'Anna, Paolo Ciambelli, Carmelo Sunseri

ISBN 978-88-95608-70-9; **ISSN** 2283-9216
DOI: 10.3303/CET1973007

Flame Aerosol Synthesis and Thermophoretic Deposition of Superhydrophilic TiO_2 Nanoparticle Coatings

Gianluigi De Falco[a]*, Mario Commodo[b], Patrizia Minutolo[b], Andrea D'Anna[a]

[a] Dipartimento di Ingegneria Chimica, dei Materiali e della Produzione Industriale - Università degli Studi di Napoli Federico II, P.le Tecchio 80, 80125, Napoli, Italy
[b] Istituto di Ricerche sulla Combustione - CNR, P.le Tecchio 80, 80125, Napoli, Italy
gianluigi.defalco@unina.it

A highly controllable and tunable technique for the production of thin coating layers of TiO_2 nanoparticles by aerosol flame synthesis and direct thermophoretic deposition is presented. Different flame reactor operations were used to study the effect of particle size and film morphology on coating performances. Particle dimension, crystal phase, coating thickness and optical properties were characterized using Scanning Mobility Particle Sizer, Raman spectroscopy and UV-Vis Absorption. Water contact angle analysis was used to investigate the wetting behavior, showing that titania coating layers are characterized by a high photoinduced hydrophilicity activated by normal solar radiation in standard room illumination conditions. The hydrophilic character was found to be dependent on the dimension of primary particles composing the coating layers. The optimal synthesis conditions have been identified in order to produce a superhydrophilic coating material.

1. Introduction

The study of novel technologies based on nanomaterials has been recently received a great interest due to its perceived potential in several science fields. Among several methods used to synthesize and to assemble specific nanoparticles into functional systems and layers, aerosol flame synthesis represents a powerful tool based on the well-established knowledge gained from traditional combustion science and technology (Li et al., 2016; Reverberi et al., 2016). Indeed, aerosol flame synthesis allows to produce nanomaterials with desired properties in an easily, cost-effectively and scalable way, and to directly deposit synthesized nanoparticles into nanostructured coatings and films by thermophoresis (Mädler et al., 2006).
One of the most attractive nanomaterials is titanium dioxide TiO_2, since it has proven to possess a high photocatalytic and antimicrobial activity (De Falco et al., 2017; Mammadov et al., 2017), as well as a low environmental and biological toxicity (McCracken et al., 2016). The photoinduced activity of TiO_2 nanoparticles is related to the formation of reactive oxygen species ROS (Fujishima et al., 2000), which in turn can result in an increase of hydrophilicity of TiO_2 coating surfaces due to the presence of hydroxyl groups, making nano-TiO_2 an ideal nanomaterial for self-cleaning antimicrobial coatings (De Falco et al., 2018).
In this paper, the production of thin coating layers of TiO_2 nanoparticles by aerosol flame synthesis and direct thermophoretic deposition is reported. Different flame reactor operation modes were used in order to study the effect of particle size on the performances of coatings, particularly in terms of hydrophilic/superhydrophilic behaviour.

2. Experimental

Titanium dioxide nanocoatings were produced using an Aerosol Flame Synthesis set-up, composed of a custom made honeycomb burner and a thermophoretic deposition system made of a rotating circular aluminium disk. The experimental set-up is similar to that described in earlier works (De Falco et al., 2017; De Falco et al., 2018), apart from the system used to feed the precursor solution to the reactor, which is now based on a high pressure syringe pump KD Scientific KDS 410. The flame synthesis and thermophoretic deposition systems are schematically described in Figure 1.

Paper Received: 04 April 2018; Revised: 15 September 2018; Accepted: 19 December 2018

Please cite this article as: De Falco G., Commodo M., Minutolo P., D'Anna A., 2019, Flame Aerosol Synthesis and Thermophoretic Deposition of Superhydrophilic Tio2 Nanoparticle Coatings , Chemical Engineering Transactions, 73, 37-42 DOI:10.3303/CET1973007

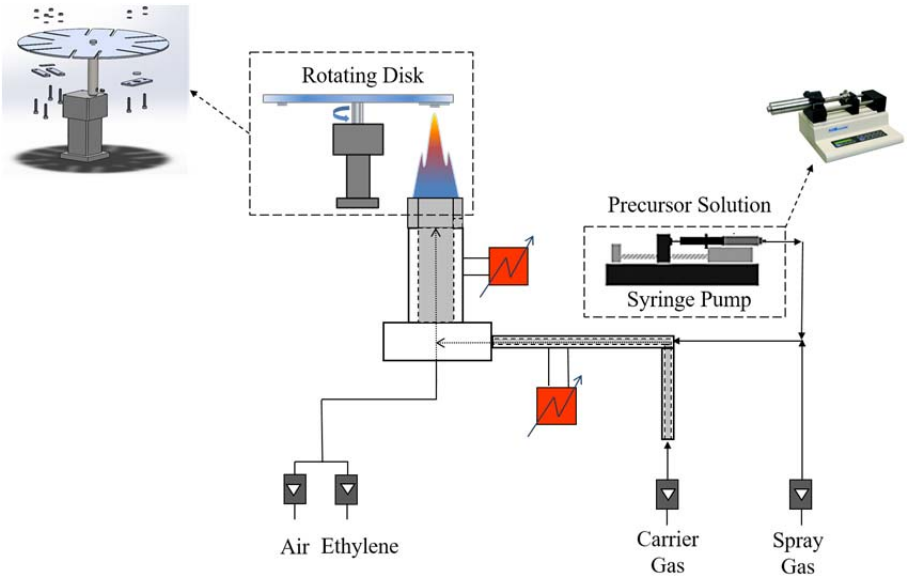

Figure 1: Schematic of the experimental set-up.

The flame reactor consists of a premixed ethylene/air laminar flame (cold gas velocity= 95 cm/s, equivalent ratio Φ=0.95) doped with solutions of titanium tetraisopropoxide (TTIP) dissolved into ethanol.
Two different flame reactor operating conditions were studied, in order to produce nanoparticles with different dimensions, by varying the TTIP concentration in the solution and the liquid flow rate of the precursor solutions, and so the amount of precursor fed to the reactor. Flame reactor main parameters are reported in Table 1.

Table 1: Summary of investigated flame conditions

Flame	C_2H_4 (Nl/hr)	Air (Nl/hr)	Spray Air (Nl/hr)	Carrier Air (Nl/hr)	TTIP Concentration (M)	Solution flow rate (μL/min)
0.5 M	36	700	40	30	0.5	900
1 M	36	700	40	30	1	600

TiO_2 nanostructured coatings were deposited onto aluminium alloy AA2024 circular substrates, 16 mm in diameter and 3 mm thick, using a rotational speed of the disk equal to 600 rpm. Coatings with different thickness were obtained by varying the total deposition time t_d.
On-line measurements of particle size distributions (PSD) were done by using a Scanning Mobility Particle Sizer (SMPS, TSI Model 3938). Measurements were performed with a horizontal probe with a 0.3 mm side pinhole, following a procedure reported elsewhere (Commodo et al., 2017). Raman spectra were acquired using a Horiba XploRA Raman Microscope System and an excitation wavelength of 532 nm. The absorption spectra of coatings were recorded with an Agilent UV–visible 8453 spectrophotometer. Static contact angle measurements was performed to analyse the wetting behaviour, by directly dropping 6 μl of bi-distilled water on the coated substrates, under ordinary light radiation in standard room illumination conditions.

3. Results and Discussion

Figure 2 reports the particle size distributions obtained by on-line SMPS measurements for the two flame conditions, together with their best fit obtained using a lognormal distribution function, whose main parameters are the mean particle diameter $<D_p>$, and the geometric standard deviation σ. From the fitting procedure, the mean particle diameter was found to increase from $<D_p>=3.2$ nm for Flame 0.5 M, with σ=1.4, to $<D_p>=18$ nm for Flame 1 M, with σ=1.1, due to the increase in precursor concentration fed to the flame reactor.

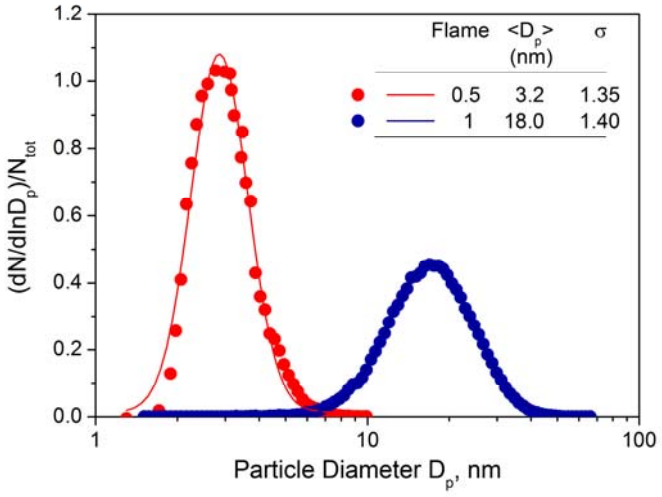

Figure 2: Normalized number particle size distributions: symbols are experimental data, lines are best lognormal fits.

Raman spectroscopy was used to identify the phase composition of flame-produced nanoparticles composing the coatings. Raman spectra acquired on Flame 0.5 M and Flame 1 M coatings shown in Figure 3, show~~ing~~ only the presence of five Raman scattering peaks corresponding to the allowed modes of anatase phase TiO_2. Coatings were made of pure anatase particles, as expected since the formation of anatase is favoured in oxygen-rich environments with respect to rutile formation (Memarzadeh et al., 2011).

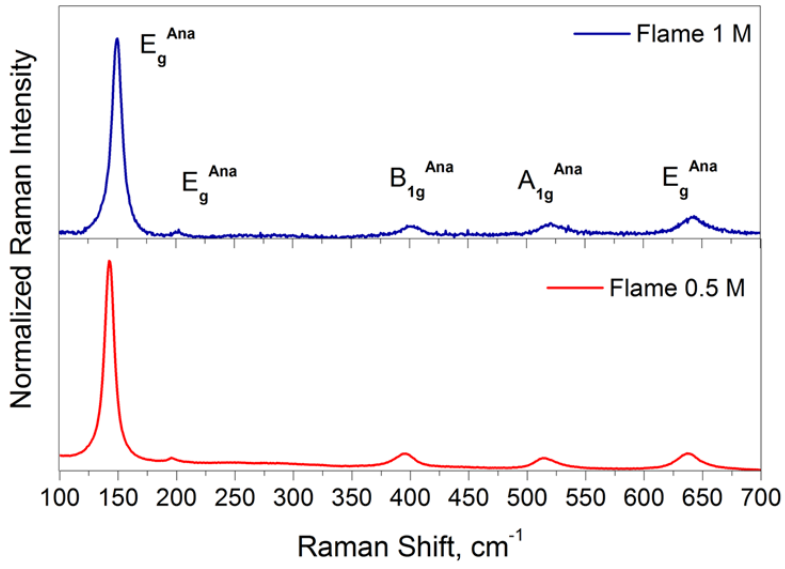

Figure 3: Raman spectra of nanostructured coatings.

The UV-visible absorption spectra were acquired on coatings produced with different deposition times. The spectra of coatings obtained from Flame 0.5 M with t_d=40 s and Flame 1 M with t_d=15 s are reported in Figure 4, showing a high absorbance in the UVA/UVB region, as well as an absorption tail in the visible region.

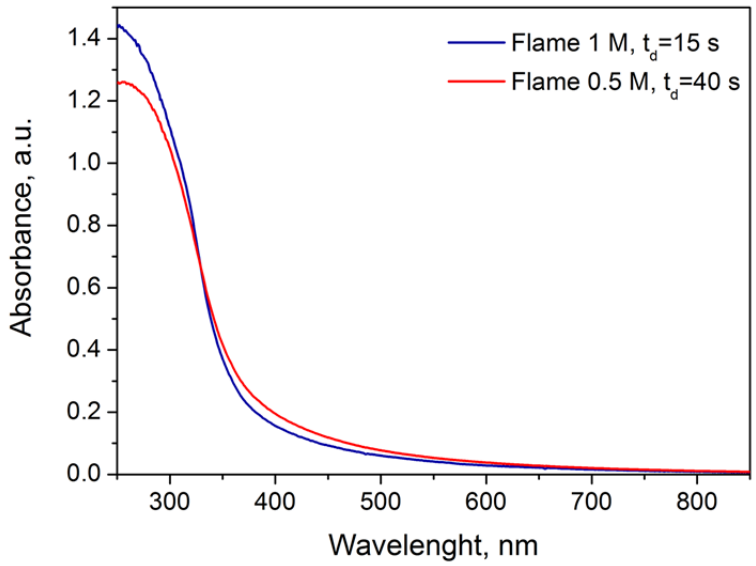

Figure 4: UV-visible absorption spectra of titania nanoparticle coatings.

From light absorbance spectrum of each coating, the bulk layer thickness of nanoparticles composing the coating, i.e., the thickness of the material in the absence of voids, can be derived using the well-known Lambert-Beer law and the refractive index of anatase particles (Mohamed et al., 2013). The bulk coating thickness obtained from UV-Vis spectra were the used to calculate the mass surface density of particle layers in each coating, i.e., the actual mass of particles in the coatings per unit area, assuming a density of anatase nanoparticles equal to 3.9 g/cm^3. The mass surface density values are shown in Figure 5a for Flame 0.5 M and Figure 5b for Flame 1 M, as a function of the deposition time.

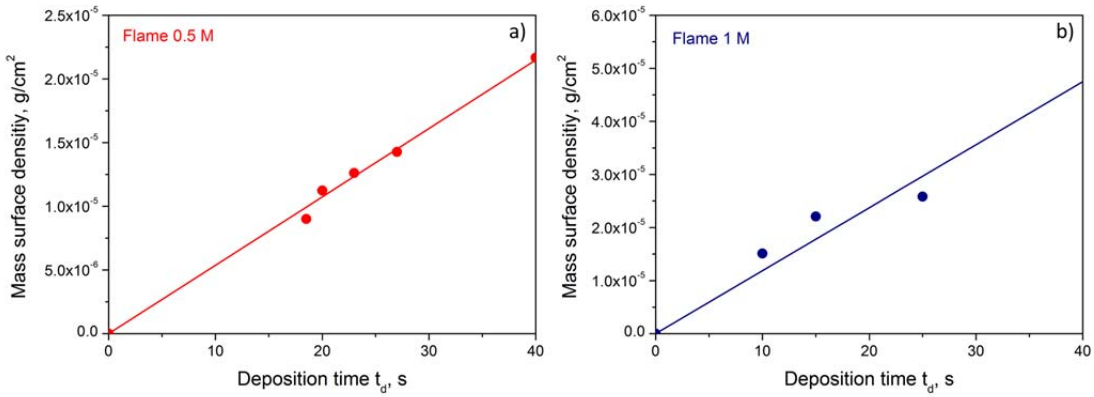

Figure 5: Calculated mass surface density as a function of deposition time for Flame 0.5 M (a) and Flame 1 M (b): dots are experimental data, lines are linear fits.

The wetting behaviour of the coatings was evaluated by water contact angle analysis. Measurements were performed firstly under ordinary light radiation in a standard room illumination condition, and then repeated on samples that had been deactivated by placing them in the dark, thus in the absence of any radiation, for 24 h, 48 h and 72 h (dark storage time). The results are reported as a function of dark storage time in Figure 6a (Flame 0.5 M) and Figure 6b (Flame 1 M) for different deposition times, and so different mass surface densities of nanoparticles in the coatings. All the generated coatings possess a hydrophilic character (contact angle < 90°) that increases as the deposition time increases. From contact angle measurements, it is possible to observe that the coatings produced in Flame 0.5 M with t_d=15 s and in Flame 1 M with t_d=15 reach a super-hydrophilic behaviour, with a measured angle equal to zero. As already reported, the high hydrophilicity of flame-synthesized TiO_2 thin films is mainly caused by a photoinduced process (Zhang et al., 1998; De Falco et

al., 2018). Measurements performed on deactivated samples confirmed the occurrence of such process, since water contact angle increases for all the samples as the dark storage time increases.

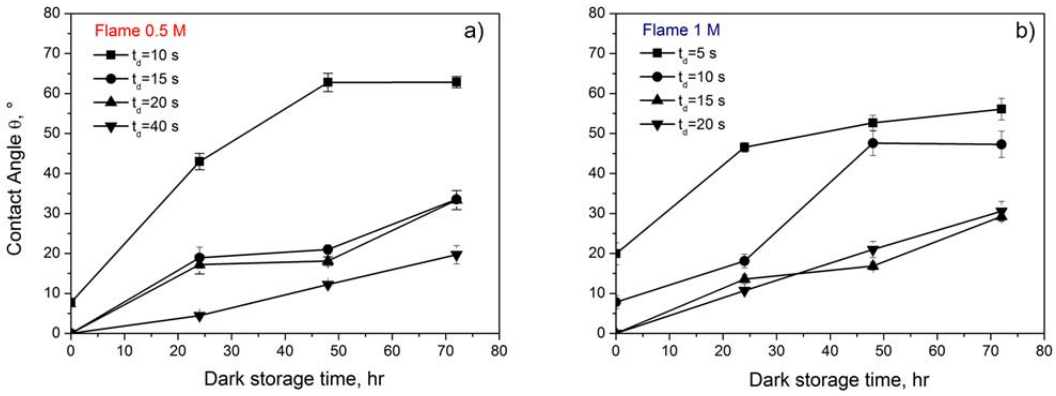

Figure 6: Water contact angles measured as a function of dark storage time for Flame 0.5 M (a) and Flame 1 M (b), at different deposition time t_d.

In order to isolate the effect of primary particle size composing the coatings on the wetting behaviour, contact angle measurements were compared between samples with the same mass surface densities made of primary particles with different sizes (<D_p>=3.2 nm for Flame 0.5 M; <D_p>=18 nm for Flame 1 M). Such a comparison is explained in Figure 7a, where measured contact angle for Flame 0.5 M t_d=15 s coating and for Flame 1 M t_d=5 s coating are reported (mass surface density ~7^{-6} g/cm^2), and Figure 7b, where measured contact angle for Flame 0.5 M, t_d=40 s coating and for Flame 1 M. t_d=15 s coating are reported (mass surface density ~2^{-5} g/cm^2). In both cases, Flame 0.5 M coatings are characterized by lower contact angles, and so a higher hydrophilic character. For Flame 0.5 M coatings, the superhydrophilic behaviour is obtained for lower mass surface density in coatings and the contact angle increase in the absence of UV-Vis radiation is slower. Those findings suggest that the lower dimension of primary particles is the driving parameter for the higher photoinduced hydrophilicity, since a reduction in particle size results in a more highly hydroxylated surface, due to the increased exposed surface area per unit volume, and so the higher number of surface active sites per photogenerated hole (Fujishima et al., 2008; De Falco et al., 2018).

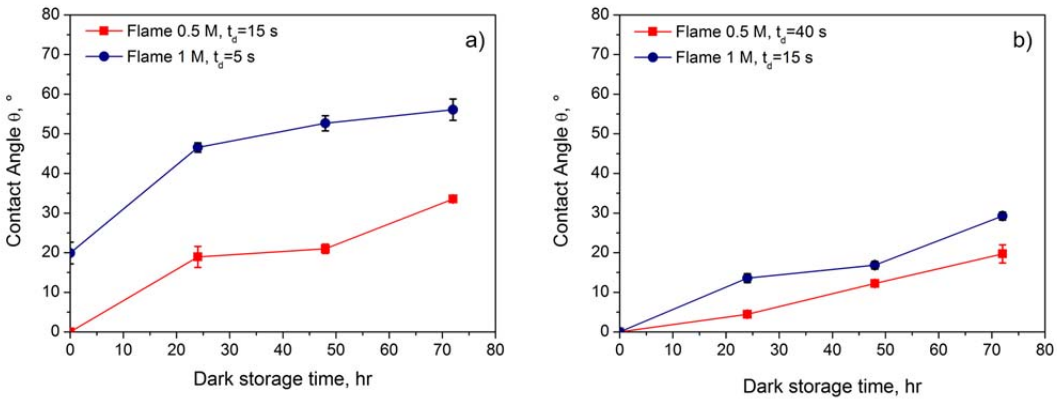

Figure 7: Water contact angles measured as a function of dark storage time for Flame 0.5 M td=15 s coating and Flame 1 M td=5 s coating (a) and for Flame 0.5 M, td=40 s coating and Flame 1 M, td=15 s coating (b).

4. Conclusions

The production of superhydrophilic TiO_2 nanostructured coatings via aerosol flame synthesis and in-situ thermophoretic deposition was presented. The system allowed to obtain pure anatase nanoparticles with controlled dimension, ranging from 3 nm to 18 nm. The coatings behaviour has been seen to depend on the

dimension of the primary particles. A minimal mass surface density of about 7E-6 g/cm^2 for 3 nm particles coatings was necessary to obtain fully superhydrophilic properties, while for coatings made of 18 nm particles coatings a minimal mass surface density of about 2E-5 g/cm^2 was necessary. Since flame-synthesized TiO_2 nanostructred coatings have already demonstrated a high antimicrobial activity (De Falco et al., 2017), the method herein presented is effective to produce nano-TiO_2 coatings that, even under ambient light irradiation, are superhydrophilic and highly antimicrobial, and so can be applied as self-cleaning and self-disinfecting nanomaterials.

References

Commodo M., D'Anna A., De Falco G., Larciprete R., Minutolo P., 2017, Illuminating the earliest stages of the soot formation by photoemission and Raman spectroscopy, Combustion and Flame, 181, 188-197.

De Falco G., Porta A., Petrone A., Del Gaudio P., El Hassanin A., Commodo M., Minutolo P., Squillace A., D'Anna A., 2017, Antimicrobial activity of flame-synthesized nano-TiO_2 coatings, Environmental Science: Nano, 4, 1095–1107.

De Falco G., Ciardiello R., Commodo M., Del Gaudio P., Minutolo P., Porta A., D'Anna A., 2018, TIO_2 nanoparticle coatings with advanced antibacterial and hydrophilic properties prepared by flame aerosol synthesis and thermophoretic deposition, Surface & Coatings Technology, 349, 830–837.

Fujishima A., Rao T.N., Tryk D.A., 2000, Titanium dioxide photocatalysis, Journal of Photochemistry and Photobiology C: Photochemistry Reviews, 1,1–21.

Fujishima A., Zhang X., Tryk D.A., 2008, TiO_2 photocatalysis and related surface phenomena, Surface Science Reports 63, 515–582.

Li S., Ren Y., Biswas P., Tse S.D., 2016, Flame aerosol synthesis of nanostructured materials and functional devices: processing, modeling, and diagnostics, Progress in Energy and Combustion Science, 55, 1–59.

Mädler L., Roessler A., Pratsinis S.E., Sahm T., Gurlo A., Barsan N., Weimar U., 2006, Direct formation of highly porous gas-sensing films by in situ thermophoretic deposition of flame-made Pt/SnO2 nanoparticles, Sensors and Actuators B: Chemical, 114, 283–295.

Mammadov G., Ramazanov M., Kanaev A., Hasanova U., Huseynov K., 2017, Photocatalytic degradation of organic pollutants in air by application of titanium dioxide nanoparticles, Chemical Engineering Transactions, 60, 241-246.

McCracken C., Dutta P.K., Waldman W.J., 2016, Critical assessment of toxicological effects of ingested nanoparticles, Environmental Science: Nano, 3, 256–282.

Memarzadeh S., Tolmachoff E.D., Phares D.J., Wang H., 2011, Properties of nanocrystalline TiO2 synthesized in premixed flames stabilized on a rotating surface, Proceedings of the Combustion Institute, 33, 1917–1924.

Mohamed S.H., El-Hagary M., Althoyaib S., 2013, Growth of undoped and Fe doped TiO_2 nanostructures and their optical and photocatalytic properties, Applied Physics A: Materials Science & Processing, 111, 1207–1212.

Reverberi A.P., Salerno M., Fabiano B., 2016, Inorganic nanoparticles synthesis by an aerosol-assisted wet chemical method, Chemical Engineering Transactions, 47, 115-120.

Zhang Z., Wang C.-C., Zakaria R., Ying J.Y., 1998, Role of particle size in nanocrystalline TiO2-based photocatalysts, The Journal of Physical Chemistry B, 102, 10871–10878.